J Solid State Electrochem (2002) 6: 412–419
DOI 10.1007/s100080100242

ORIGINAL PAPER

C.F. Zinola · J. Rodríguez

Tin underpotential deposition on platinum and its catalytic influence on the kinetics of molecular oxygen electroreduction

Received: 26 April 2001 / Accepted: 16 July 2001 / Published online: 27 October 2001

Abstract The formation and dissolution of tin ad-layers on polycrystalline platinum were analysed by cyclic voltammetry in aqueous 10^{-4} M tin(II)/1 M sulfuric acid in the 0.05–0.70 V versus RHE range. At this concentration level it was possible to observe that platinum sites involving (110) planes are mainly related to tin underpotential deposition. In contrast to previous results, no irreversible adsorption was found in the course of the electrodeposition. Thermodynamic adsorption parameters were calculated from the potential dependence of tin surface coverage. Catalytic properties of this new surface were studied on the basis of oxygen electroreduction as a model. Kinetic runs were performed with rotating ring-disk electrodes on bare and tin-modified platinum surfaces. Molecular oxygen reduction on tin-modified platinum takes place through the production of both water and hydrogen peroxide. This interpretation was confirmed by calculating the reaction order with respect to oxygen.

Keywords Underpotential deposition · Platinum · Tin · Oxygen electroreduction

Introduction

The low oxidation potential of tin makes it an interesting material for oxidative catalytic processes [1, 2, 3, 4, 5]. In spite of several papers published on tin deposition [1, 2, 4], the overlapping of underpotential (UPD) and bulk processes under certain conditions obscures data analysis. Tin UPD on stepped single crystal platinum [Pt(332) and Pt(755)] has been investigated as possible substitutes for hydrogen adatoms [1, 2]. Interesting catalytic effects of tin adatoms on polycrystalline (pc) platinum surfaces have been advanced [6, 7] for formic acid and carbon monoxide electrooxidations.

In certain experimental conditions, tin UPD deposition on platinum occurs through an irreversible adsorption, forming bimetallic compounds such as [Pt_3Sn] and [PtSn] with different catalytic activities compared to a reversible process [8]. On the other hand, it has been found [8, 9] that the adsorption of a tin monolayer from soluble species in aqueous hydrochloric acid yields unstable films on gold. In the case of palladium electrodes, adsorption of tin also takes place by the ionization of hydrogen adsorbates together with an irreversible disproportionation of tin(II), producing tin(IV) and adsorbed tin(0) species, making the interpretation more difficult [10, 11]. In this sense, it has been shown by Mössbauer spectroscopy [7] that there is no difference between tin UPD and bulk deposition processes on metal surfaces. However, Cadle and Brückenstein [8] have found a preferred occupation site by the foreign metal when atomic radii of this metal (tin) and the substrate (platinum) are similar. The result is the inhibition of a particular type of platinum-hydrogen interaction. However, Motoo and Furuya [10] have postulated a rearrangement for copper UPD on platinum from disordered to ordered structures with the simultaneous appearance of free platinum sites even in the case of having more than one monolayer. To envisage this effect, a potentiodynamic cycling after tin deposition on platinum was applied in this work within the region involving the operative deposition potentials.

One of the most important electrocatalytic process on platinum is the oxygen electroreduction reaction (OERR); however, high overpotentials are required for developing noticeable current densities [12, 13]. OERR rates can be increased using alternative electrolytes or by changing adequately the electrode surface composition [14, 15]. In this sense, the electrochemistry at UPD levels of different metals on noble electrodes has been one of the most attractive topics in electrocatalysis [16, 17]. Copper has been the subject of different studies at UPD levels on platinum in acid media [18, 19], and the OERR

C.F. Zinola (✉) · J. Rodríguez
Laboratorio de Electroquímica Fundamental,
Facultad de Ciencias, Universidad de la República,
Avda. Libertad No. 2497, C.P. 11300, Montevideo, Uruguay
E-mail: fzinola@fcien.edu.uy

kinetics showed a strong inhibition of the 4-electron pathway in favour of the 2-electron one [18]. The OERR on platinum in aqueous solutions has been explained by a mechanism involving two parallel reactions [20, 21, 22, 23]. The first path consists of a direct 4-electron transfer reduction of molecular oxygen to water and the second involves a 2-electron transfer reduction leading hydrogen peroxide, which can be either electroreduced to water or diffused to the bulk. The relative contribution of each pathway to the net reaction depends on the experimental conditions [22, 23].

The aim of this work is to study tin UPD on pc platinum after conducting a potentiodynamic cycling within the hydrogen adsorption region and to obtain a deeper insight into the catalytic influence on OERR kinetics in acid solutions.

Experimental

Pc platinum disk working electrodes were polished to a mirror finish using alumina pastes of different grades and subsequently immersed in a 1:1 pure nitric/sulfuric acid mixture for 1 h. The real surface area was estimated from the voltammetric hydrogen-adatom charge at 0.10 V s^{-1} after double layer correction [24]. A large-area platinum plate counter electrode (50 cm^2 in geometric area) facing the disk electrode and a reversible hydrogen reference electrode (RHE) in the same electrolyte were employed. All potentials in the text are given on the RHE scale and all experiments were performed at 25 °C. Purified sulfuric acid (Merck, 98.6%), tin(II) nitrate (Sigma) and Millipore MilliQ water were used to prepare the aqueous solutions. Before each electrochemical measurement the cleanliness of the system was checked by cyclic voltammograms run at 0.10 V s^{-1} in the 0.05–1.50 V range. Negligible voltammetric changes were found after holding the potential at 0.60 V for 10 min.

Tin deposition was conducted by applying a constant deposition potential (E) ranging between 0.05 and 0.70 V in 10^{-4} M tin(II) + 1 M sulfuric acid (working electrolyte) during $t = 5$ min. Secondly, the working electrolyte was exchanged by oxygen-free 1 M sulfuric acid (supporting electrolyte) and the potential cycled in the hydrogen sorption region to obtain the stable tin surface coverage (θ_{Sn}). The values of θ_{Sn} were evaluated as explained in the Results section.

OERR kinetic runs were conducted using the rotating ring-disk electrode technique in oxygen (99.99% purity AGA) saturated supporting electrolyte. The disk potential (E_D) was scanned from 1.0 V to 0.05 V at 0.01 V s^{-1} and the ring potential (E_R) held at 1.20 V to electrooxidize the hydrogen peroxide produced on the disk under a mass-transport regime. Values of disk (I_D) and ring (I_R) currents were recorded at different rotation rates (ω) in the 500–4000 rpm range. The collection efficiency of the ring-disk device was $N = 0.22$, which was checked with the $Fe(CN)_6^{3-}/Fe(CN)_6^{4-}$ redox couple in dilute alkaline media. Since kinetic experiments involved potentials greater than ca. 0.8 V, θ_{Sn} values were controlled between each run to obtain the real surface coverage value.

Results

Cyclic voltammograms of tin UPD on pc platinum in acid solutions

Tin deposition was conducted in the working electrolyte by applying a constant potential E from 0.70 V down to 0.05 V. The equilibrium potential of the tin/tin(II) system in the working electrolyte was –0.414 V; however, the UPD process is only observed in the 0.05–0.70 V range. Below 0 V, irreversible adsorption of tin together with the hydrogen evolution reaction was observed.

The first voltammetric profile of tin UPD on pc platinum in the supporting electrolyte does not exhibit a defined shape. SEM micrographs of tin UPD formed at 0.05 V show islands with different morphologies (Fig. 1). Repetitive and reproducible current versus potential profiles can be obtained only after applying at least 10 cycles in the 0.05–0.60 V range (dotted lines in Fig. 2). This potential cycling acts as a surface stabilization of the deposition. It is interesting to observe the different and subsequent stages during cycling tin UPD in the hydrogen sorption region (Fig. 3). The anodic charge under peak II [involving (110) crystallographic sites] abruptly diminishes, whereas peak III increases in a much lower proportion. This fact suggests that tin deposition is preferentially achieved on (110) sites and some hydrogen species rearrange to (100) sites as a consequence of deposition. Moreover, a little decrease in peak I is observed. SEM micrographs exhibit a rectangular order, together with some globular-shaped morphology (Fig. 4).

Steady state values of θ_{Sn} at any E can be calculated either from the consumed hydrogen charge by tin adsorption (Q_H) or from the voltammetric desorption charge of tin UPD (Q_{Sn}). In the first case, the ratio is between Q_H and that of saturation ($Q_H°$):

$$\theta_{Sn} = \frac{Q_H}{Q_H^\circ} \tag{1}$$

In the second case, the number of platinum sites per tin and the number of electrons involved in the oxidative desorption have to be considered. Taking into account literature data [2], a single tin atom requires two platinum atoms for UPD on pc platinum surfaces. In this

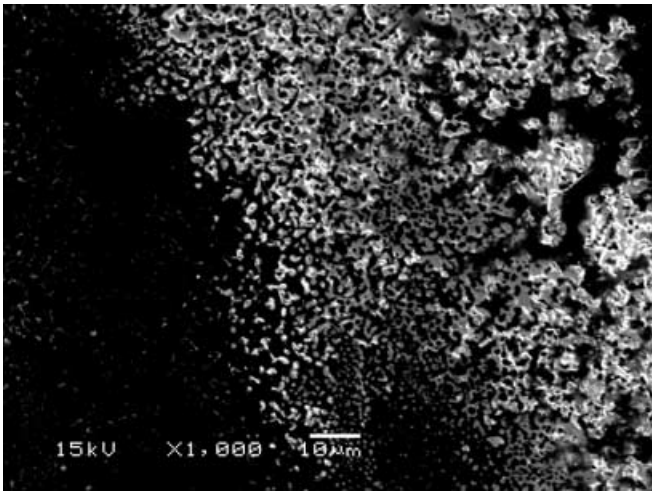

Fig. 1 SEM micrographs of tin UPD deposited at 0.05 V during 5 min in the working electrolyte. The scale is indicated in the text

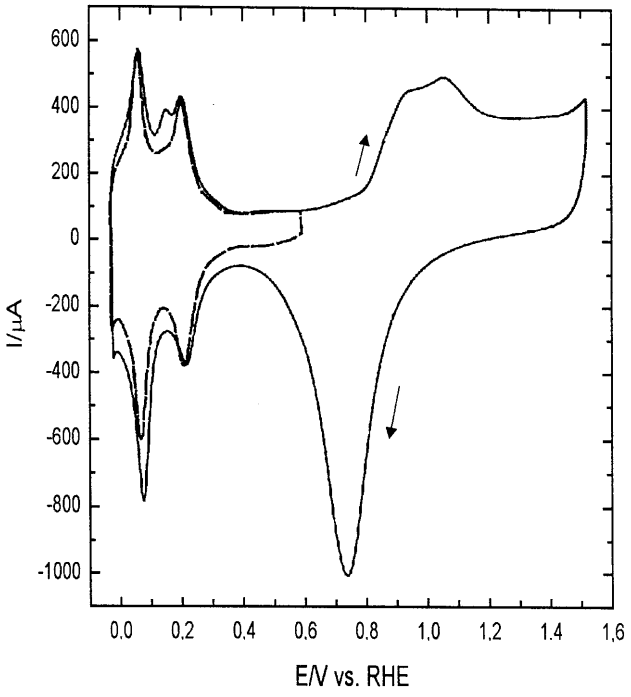

Fig. 2 Cyclic voltammograms of a pc platinum wire in supporting electrolyte within the 0.05–1.50 V (*full line*) and 0.05–0.60 V ranges after tin UPD at $\theta_{Sn} = 0.18$ (*dotted line*). $T = 25$ °C, $v = 0.10$ V s^{-1}, real area = 2.86 cm^2. *Arrows* indicate the cycling direction. Tin deposition was performed in the working electrolyte at 0.62 V during 5 min

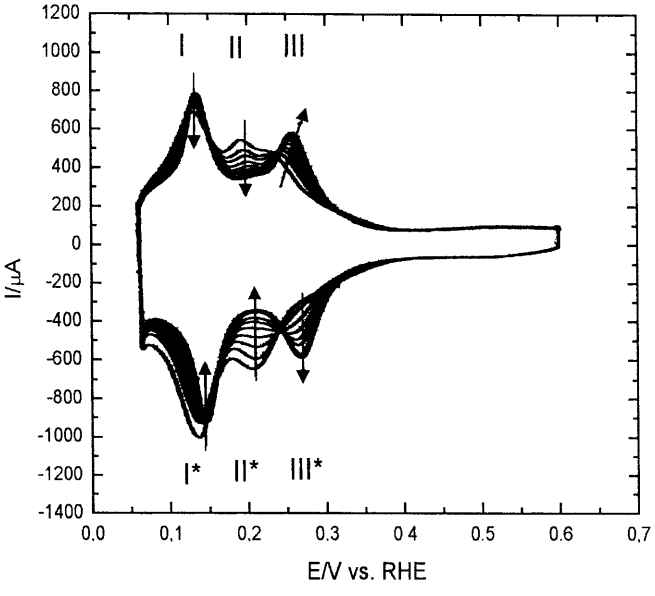

Fig. 3 Subsequent voltammetric cycles between 0.05 V and 0.60 V for tin UPD ($\theta_{Sn} = 0.18$) on a pc platinum wire in supporting electrolyte. Real area = 4.52 cm^2, $T = 25$ °C, $v = 0.10$ V s^{-1}. *Arrows* indicate cycling effects on the voltammetric profile. Anodic peaks are labeled as I, II and III and cathodic peaks as I*, II* and III*

case the anodic desorption profile is integrated from E up to 1.1 V, considering the complete formation of tin(II) species. Then:

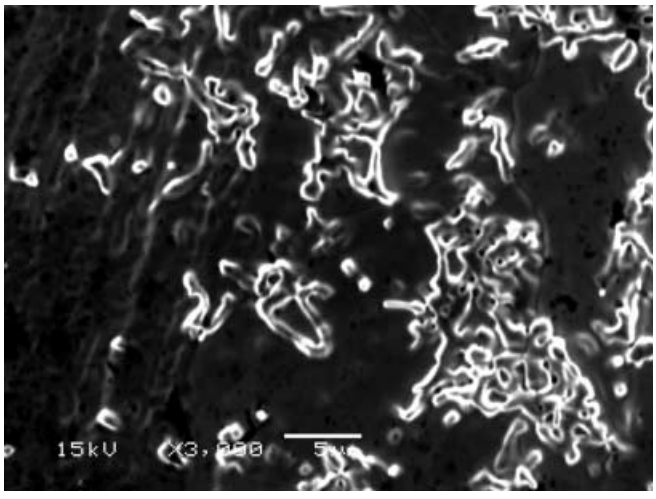

Fig. 4 SEM micrographs of tin UPD obtained at 0.05 V during 5 min in the working electrolyte after 10 cycles run at $v = 0.10$ V s^{-1} in the 0.05–0.60 V range. Scales are indicated in the text

$$\theta_{Sn} = \frac{Q\mathrm{Sn}}{2Q_H^o} \tag{2}$$

The calculation of θ_{Sn} from Eqs. 1 and 2 yields equivalent values (±5%).

To properly evaluate Q_{Sn}, E was firstly held at 1.50 V during 10 s to eliminate any traces of tin on the surface, then stepped to a fixed value for 5 min, and finally a fast anodic scan (more than 0.250 V s^{-1}) was applied from the preset potential to 1.50 V and recorded in an oscilloscope. This fast anodic sweep avoids any further tin deposition. The integration of the current versus potential profile defines Q_{Sn}. The electrodissolution of the tin UPD layer shows three desorption peaks at ca. 0.3, 0.5 and 0.75 V, whose relative contributions vary according to the values of Q_{Sn}. At low θ_{Sn} values, only one desorption peak is observed at 0.72 V (Fig. 5), but from $\theta_{Sn} = 0.2$ to 0.66 (saturation), three peaks are well defined.

The possibility of tin(II) disproportionation to tin(IV) and tin(0) was also checked in the working electrolyte using the following procedure. First, the cyclic voltammogram of pc platinum in the supporting electrolyte was obtained as explained in the Experimental section. Then, the electrolyte was exchanged with the working electrolyte, which was completely freed from dissolved oxygen to reach the open circuit potential after ca. 5 min. After this time the electrode was rinsed with supporting electrolyte again and the voltammogram determined at 0.10 V s^{-1}, scanning from this open circuit value. The resulting profile was practically the same as that firstly obtained for the pc platinum electrode in the supporting electrolyte. This result clearly shows that tin adsorption from tin(II) solutions does not occur at open circuit, contrary to experiments at higher solution concentration levels.

Motoo and Furuya [10] demonstrated that tin UPD on platinum inhibits further adsorption of hydrogen

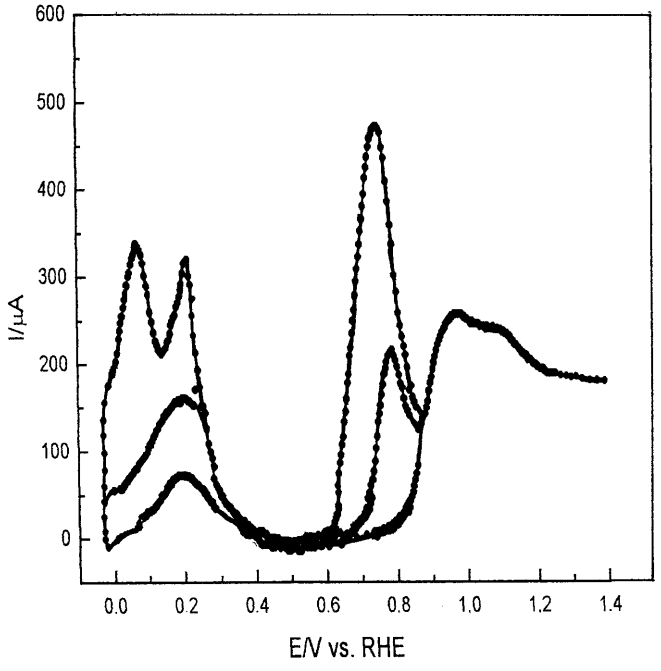

Fig. 5 Anodic stripping of tin UPD at pc platinum in supporting electrolyte. Tin deposition was performed at 0.40 V during 3 and 5 min in the working electrolyte and the voltammetric stabilization was performed as explained in the text. $T = 25$ °C, $v = 0.10$ V s^{-1}. The potential was swept first in the negative direction and then positively up to 1.4 V

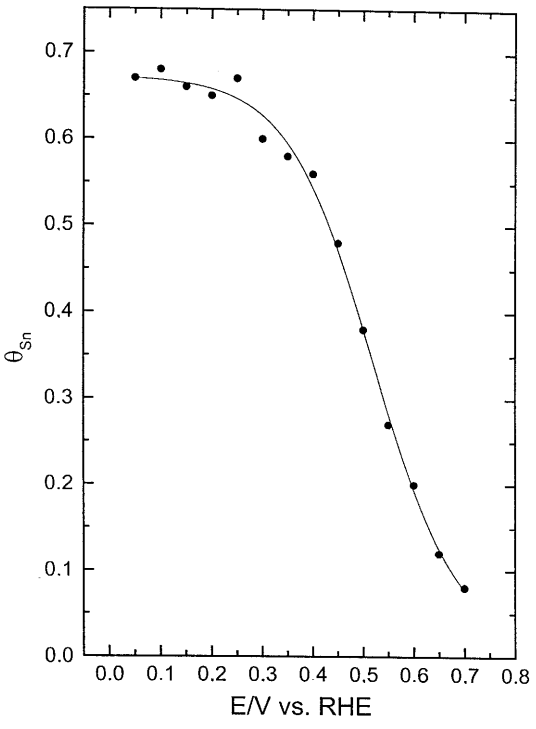

Fig. 6 θ_{Sn} versus E plot (*points*) on pc platinum in supporting electrolyte at 25 °C. The charges involved in the process were voltammetrically calculated as described in the text. Each point results from the voltammetric stabilization at $v = 0.10$ V s^{-1} (10 cycles) in the 0.05–0.60 V range. The *full-line curve* depicts the numerical fitting of a Temkin isotherm

species. They plotted the surface coverage by hydrogen ad-atoms (θ_H) as a function of $1–\theta_{Sn}$ to prove this assumption through a linear behaviour. In the case of this paper, a similar situation was demonstrated; however, a surface rearrangement by potentiodynamic cycling was observed (Fig. 2). Therefore, any further conclusions about the structure of tin layers on platinum have to be taken with care.

Data in Fig. 6 (dots) shows the values of θ_{Sn} plotted as a function of E after voltammetric stabilization in the 0.60 V to 0.05 V range. The isotherm exhibits a typical sygmoidal shape, i.e. a slow increase in θ_{Sn} between 0.70 and 0.45 V, before attaining saturation ($\theta_{Sn} = 0.66$) from 0.25 to 0.05 V.

It is important to establish the type of isotherm by numerical fitting. Thus, a Temkin adsorption isotherm for tin UPD on platinum was assayed and is represented in Fig. 6:

$$\left(\frac{\theta_{Sn}}{1-\theta_{Sn}}\right)\exp\left(\frac{r\theta_{Sn}}{RT}\right) = a_{Sn^{2+}}\exp\left(\frac{-\Delta G^{O}_{ad,\theta=0}}{RT}\right)\exp\left(\frac{-nFE}{RT}\right) \quad (3)$$

where $n = 2$ is the number of electrons involved in the UPD process, a_{Sn2+} is the activity referred to a 10^{-4} M tin(II) concentration, $\Delta G^{\circ}_{ad,\theta=0}$ is the standard free energy of adsorption at zero surface coverage, and the rest of the symbols have their usual meanings.

Linearizing Eq. 3 at constant potential, it is possible to obtain thermodynamic parameters ($\Delta G^{\circ}_{ad,\theta=0}$ and r):

$$\ln\left(\frac{\theta_{Sn}}{1-\theta_{Sn}}\right) = \ln A - \frac{r\theta_{Sn}}{RT} \quad (4)$$

with:

$$\ln A = \ln\left(a_{Sn^{2+}}\right) - \frac{\Delta G^{\circ}_{ad,\theta=0}}{RT} - \frac{nFE}{RT} \quad (5)$$

Then, by plotting $\ln(1–\theta_{Sn})/\theta_{Sn}$ versus θ_{Sn} at each E, we can obtain the value of r from the slope and the value of $\Delta G^{\circ}_{ad,\theta=0}$ from the ordinate at $\theta = 0$.

Since (110) sites seem to be directly involved in tin UPD process, we have constructed a $\ln(1–\theta_{Sn})/\theta_{Sn}$ versus θ_{Sn} plot considering only the charge involving peak II separately from the entire tin UPD region. A single value of $\Delta G^{\circ}_{ad,\theta=0}$ is obtained from both curves: -420 ± 40 kJ mol^{-1}. This means that tin UPD is governed mainly by the interaction of the metal with (110) sites.

The value of r in the Temkin isotherm defines interactions between hydrogen and tin ad-atoms:

$$\Delta G^{\circ}_{ad,\theta=0} = \Delta G^{\circ}_{ad,\theta=0} + r\theta_{Sn} \quad (6)$$

$$r = \left(\frac{\partial \Delta G^{\circ}_{ad,\theta}}{\partial \theta_{Sn}}\right)_{T,E} \quad (7)$$

In spite of the similar value of $\Delta G^{\circ}_{ad,\theta=0}$ obtained in each case, the evaluation of r leads to different results, as expected: $r = 13$ kJ mol^{-1} for the entire UPD domain and $r_{(110)} = 42$ kJ mol^{-1} for the charge under peak II. These values of r cover the experimental error of $\Delta G^{\circ}_{ad,\theta=0}$ and do not change significantly for increasing θ_{Sn}. Since the results showed a small positive value of r, a rather small attraction between hydrogen and tin adatoms is expected on the surface.

Figure 7 shows the first differentiation of the θ_{Sn} versus E plot. A slow decrease of the ordinate with potential is observed until the minimum is reached at $E(\theta_{sat}/2) = 0.55$ V. This potential should be treated as the standard potential of the UPD process, leading to a constant value which only depends on the supporting electrolyte, ion concentration and temperature.

Rotating ring-disk voltammograms for the OERR on tin UPD pc platinum in sulfuric acid solutions

The I_D versus E_D and I_R versus E_D rotating voltammograms for the OERR were recorded in oxygen-saturated supporting electrolyte on pc platinum and on tin UPD platinum (Fig. 8). The selected rotation speeds were $\omega = 500$, 1000, 2000, 3000 and 4000 rpm.

The I_D versus E_D and I_R versus E_D voltammograms for the OERR on bare platinum are shown in Fig. 8a. Non-zero currents for the disk electrode were observed from 0.80 V downwards, and the general contour exhibits the normal response of a mixed controlled reaction.

The kinetics of the OERR at platinum surfaces modified by tin UPD exhibits different characteristics. Figure 8b shows the voltammogram for $\theta_{Sn} = 0.48$ with two limiting currents, one due to oxygen electroreduction (I_D versus E_D) and another due to hydrogen peroxide oxidation (I_R versus E_D). It is important to emphasize that the appearance of a limiting current on both voltammograms is an indication that OERR kinetics is not totally blocked by tin; in other words, tin layers are more likely structured as islands than as flat sub-monolayers. Both limiting currents vary linearly with the square root of ω, as expected from the Levich equation. Comparing the curves with those obtained for the OERR at bare platinum, no contributions of peroxide adsorbates in the I_R versus E_D voltammogram were observed.

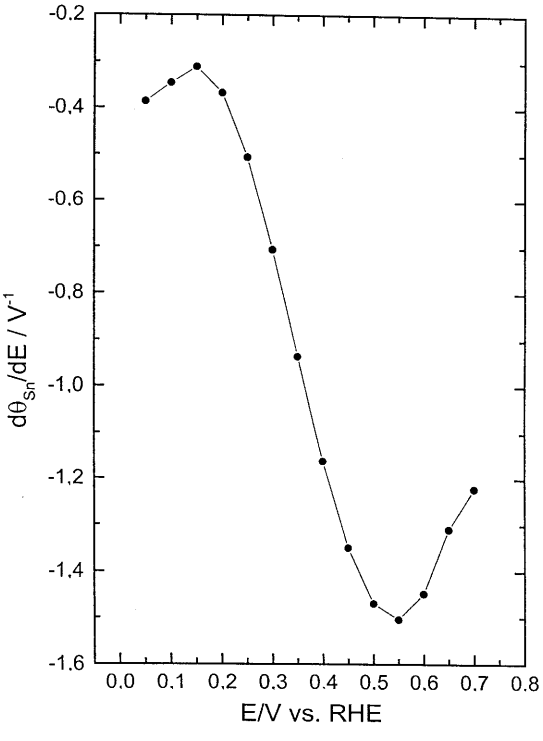

Fig. 7 $\partial\theta_{Sn}/\partial E$ versus E plot on pc platinum in supporting electrolyte at 25 °C. The curve was constructed from the Temkin isotherm

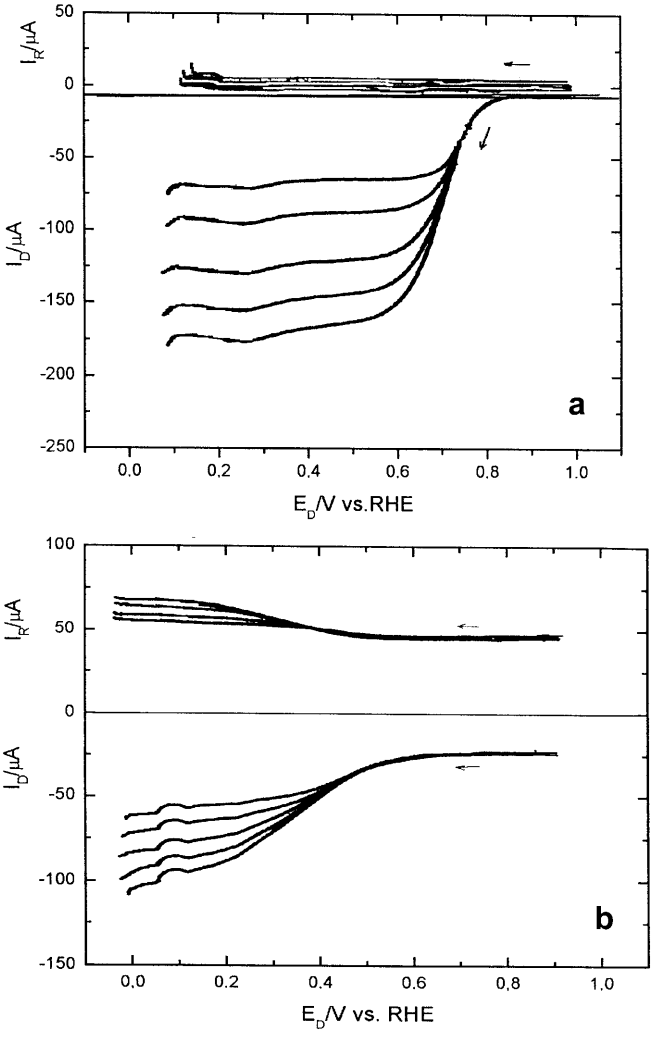

Fig. 8 I_D versus E_D and I_R versus E_D voltammograms recorded **a** at pc platinum and **b** at tin UPD platinum ($\theta_{Sn} = 0.48$) in oxygen-saturated supporting electrolyte. $T = 25$ °C; rotation speeds $\omega = 500$, 1000, 2000, 3000 and 4000 rpm; $v = 0.010$ V s^{-1}; $E_R = 1.20$ V. *Arrows* indicate the scan direction

The results for the OERR on tin UPD platinum differ from those earlier found on copper UPD at platinum in acid media [18], since no further OERR inhibition by tin is observed below a certain potential. Moreover, the maximum (saturation) value of θ_{Sn} is not 1 but 2/3, indicating the presence of free platinum sites available for the OERR. The results found from the kinetics of the OERR at tin-modified surfaces clearly show that this metal has a better ability to electrogenerate hydrogen peroxide because of tin partial surface blockage.

Reaction orders with respect to oxygen at tin UPD pc platinum in sulfuric acid solutions

A $\log(I_D/I_k)$ versus $\log(1–I_D/I_{LD})$ plot can be used to evaluate the reaction order with respect to oxygen, p, at constant E_D, with I_k and I_{LD} being the kinetic and limiting diffusion disk currents, respectively. The value of p found for the OERR at pc platinum in the supporting electrolyte was 0.5 ± 0.1 (Fig. 9a). On the other hand, for the OERR at tin UPD platinum, p was 1.0 ± 0.1, independent of θ_{Sn} (Fig. 9b). These values were expected because the formation of solution hydrogen peroxide was demonstrated by rotating ring-disk voltammograms at tin UPD platinum.

Fractional reaction orders for the OERR were found in the literature for an oxygen dissociation process producing atomic oxygen on pc platinum in aqueous acid [13, 14]. The value of p of nearly 1, independent of θ_{Sn}, denotes a strong influence of this metal on the OERR. Similar results have been found before for the OERR on (100) preferentially oriented platinum in trifluoromethanesulfonic acid [21].

It is usual to corroborate the values of p by plotting the Koutecký-Levich expression with the substitution of the appropriate reaction orders:

$$\frac{I_D}{I_k} = \left(1 - \frac{I_D}{I_{LD}}\right)^p \tag{8}$$

For $p = 1$, we have:

$$\frac{1}{I_D} = \frac{1}{I_k}\left(\frac{I_{LD}}{I_{LD} - I_D}\right) \tag{9}$$

and for $p = 1/2$:

$$\frac{I}{I_D} = \frac{I}{I_k}\left(\frac{I_{LD}}{I_{LD} - I_D}\right)^{1/2} \tag{10}$$

After conducting the appropriate substitutions in Eqs. 9 and 10, a coincidence with p obtained from $\log(I_D/I_k)$ versus $\log(1–I_D/I_{LD})$ plots within 15% was observed.

The experimental Levich slope, B_{exp}, was calculated for the OERR at pc platinum. The correspondence between $B_{exp} = 0.033 A_D$ (mA $s^{-1/2}$) and B, the theoretical Levich slope, makes our calculations of p reliable. The value of B is related to $I_{LD} = B\omega^{1/2}$ with $B = 0.62nFC^{\circ}_{O2}D^{2/3}_{O2}v^{-1/6}A_D$, A_D being the geometric disk surface area. The other symbols have their usual meaning.

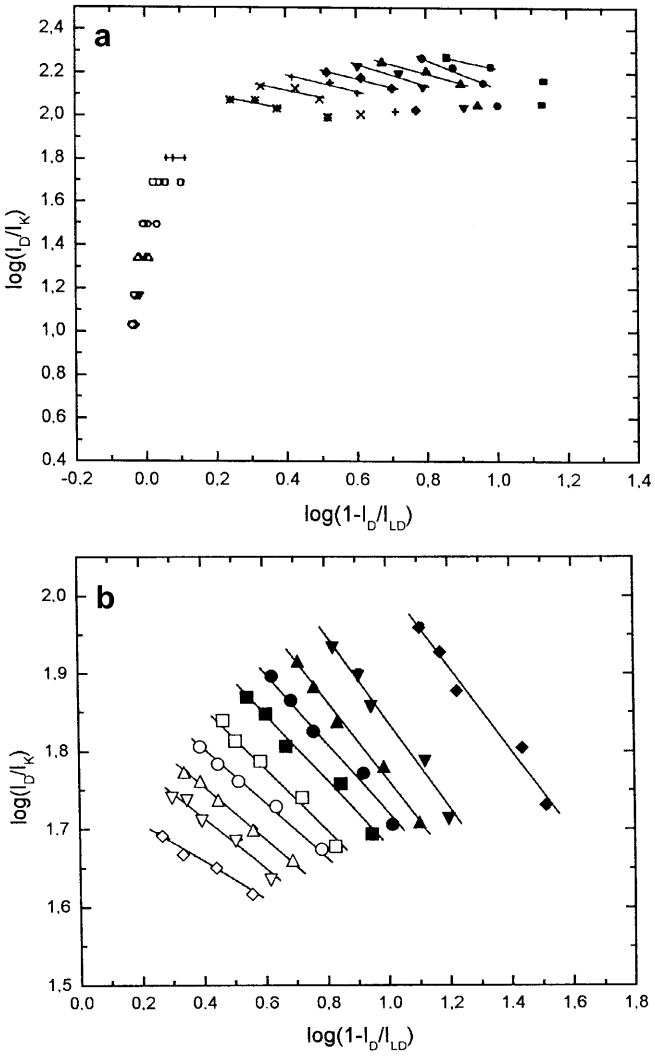

Fig. 9 $\log(I_D/I_k)$ versus $\log(1–I_D/I_{LD})$ plots **a** at pc platinum and **b** at tin UPD platinum ($\theta_{Sn} = 0.48$) in oxygen-saturated supporting electrolyte. $T = 25$ °C; *filled squares*: 0.60 V; *filled circles*: 0.62 V; *filled up triangles*: 0.64 V; *filled down triangles*: 0.66 V; *filled diamonds*: 0.68 V; *plus signs*: 0.70 V; *crosses*: 0.72 V; *asterisks*: 0.74 V; *vertical lines*: 0.76 V; *open squares*: 0.78 V; *open circles*: 0.80 V; *open squares*: 0.82 V; *open up triangles*: 0.84 V; *open down triangles*: 0.86 V; *open diamonds*: 0.88 V, *plus signs*: 0.90 V

Discussion

Among all reaction schemes, the one proposed by Damjanovic et al. [20, 22] has been successfully applied to study OERR kinetics on platinum metals in aqueous solutions. This scheme considers global series and parallel reaction pathways, comprising a direct oxygen electroreduction to water (path 1), a parallel electroreduction to hydrogen peroxide (path 2) and a further electroreduction of hydrogen peroxide to water (path 3). Each one of these steps is characterized by

electrochemical reaction rates, usually named $\overline{k_1}$, $\overline{k_2}$ and $\overline{k_3}$, respectively. The rotating ring-disk technique is commonly used to discern whether hydrogen peroxide is produced either as an intermediate adsorbate or as product in the OERR mechanism. Then, Damjanovic's scheme predicts the following relationships between I_D, I_R, I_{LD} and ω:

$$\frac{I_{LD}}{I_{LD}-I_D}=1+\frac{\overline{k_1}+\overline{k_2}}{Z_1}\frac{1}{\sqrt{\omega}}$$
$$\text{where } Z_1\equiv 0.62D_{O2}^{2/3}\nu^{-1/6}\quad\text{(Levich slope)} \tag{11}$$

$$\frac{I_D}{I_R}=\frac{1}{N}\left(1+\frac{2\overline{k_1}}{\overline{k_2}}\right)+\left[\frac{2\overline{k_3}\left(1+\overline{k_1}/\overline{k_2}\right)}{NZ_2}\right]\frac{1}{\sqrt{\omega}}$$
$$\text{where } Z_2\equiv 0.62D_{H2O2}^{2/3}\nu^{-1/6} \tag{12}$$

If p was really equal to 1, Eq. 11 would predict $I_{LD}/(I_{LD}–I_D)\rightarrow 1$ at $\omega^{-1/2}\rightarrow 0$. Besides, the linear behaviour suggests a negligible hydrogen peroxide chemical decomposition. If this does not apply, Wroblowa's scheme can be used [14, 23].

I_D/I_R versus $\omega^{-1/2}$ and $I_{LD}/(I_{LD}–I_D)$ versus $\omega^{-1/2}$ plots for the OERR at pc and tin UPD platinum were constructed in the supporting electrolyte to obtain the rate constants for Damjanovic's scheme. This analysis is usually not covered since I_R values are negligible on platinum in acid solutions.

The values of S_1 (the slopes of I_D/I_R versus $\omega^{-1/2}$ plots) strongly depend on E_D for the OERR at bare platinum. On the other hand, I_1 values (the intercepts in I_D/I_R versus $\omega^{-1/2}$ plots) are large and potential dependent at bare platinum. The larger the E_D, the higher the values of I_1 and S_1. As was expected, at E_D greater than 0.84 V the value of I_1 becomes equal to $1/N\approx 3$–5, and the direct electroreduction to water is no longer present, because peroxide formation is catalysed by the presence of platinum oxides. On the other hand, the electrochemical behaviour of I_D/I_R versus $\omega^{-1/2}$ plots in the case of tin UPD defines small and potential-independent values of I_1 and small values of S_1.

The intercept (I_2) of the $I_{LD}/(I_{LD}–I_D)$ versus $\omega^{-1/2}$ plot was exactly 1 for the OERR at bare platinum and slightly larger than 1 at tin UPD platinum. On the other hand, S_2, the slope of $I_{LD}/(I_{LD}–I_D)$ versus $\omega^{-1/2}$ plots, is large and dependent on E_D at bare platinum, because of the larger production of bulk hydrogen peroxide. In case of tin UPD, the OERR defines $I_{L,D}/(I_{L,D}–I_D)$ versus $\omega^{-1/2}$ plots with small values of S_2. The values of S_2, I_1 and S_1 can be calculated from Eqs. 11 and 12:

$$S_2=\frac{\overline{k_1}+\overline{k_2}}{Z_1},\ I_1=\frac{1}{N}\left(1+\frac{2\overline{k_1}}{\overline{k_2}}\right)\text{ and }S_1=\left[\frac{2\overline{k_3}\left(1+\overline{k_1}/\overline{k_2}\right)}{NZ_2}\right] \tag{13}$$

From them, the following equations offer $\overline{k_i}$ values at different E_D:

$$\overline{k_1}=\frac{Z_1S_2(I_1N-1)}{(I_1N+1)},\ \overline{k_2}=\frac{2Z_1S_2}{(I_1N+1)},\ \overline{k_3}=\frac{NZ_2S_1}{(I_1N+1)} \tag{14}$$

Table 1 depicts the values of the three rate constants for the OERR at bare and tin UPD platinum for $\theta_{Sn}=0.48$. The OERR at bare platinum in oxygen-saturated supporting electrolyte exhibits the largest value of $\overline{k_1}$, which decreases monotonously with E_D. On the other hand, the values of $\overline{k_2}$ and $\overline{k_3}$ are, in the same solution, respectively 100 and 1000 times lower than $\overline{k_1}$ at all E_D, reaching maximum values at 0.72 V. At E_D larger than 0.80 V, $\overline{k_1}$ became nearly zero due to the catalytic formation of hydrogen peroxide at the oxidized surface.

However, the mechanism of the OERR obeyed at tin UPD platinum with θ_{Sn} values ranging from 0.10 to 0.66 is rather different. The values of $\overline{k_1}$ are 100 times higher than $\overline{k_2}$, reaching a maximum value at 0.30 V. Besides, the values of $\overline{k_2}$ are 10 times higher than those for the OERR at bare platinum, indicating a larger proportion of hydrogen peroxide in solution. Moreover, the values of $\overline{k_3}$ are similar to those found on bare platinum,

Table 1 Potential dependence of the electrochemical rate constants for the OERR at bare pc platinum (*left*) and at tin UPD ($\theta_{Sn}=0.48$) platinum (*right*) in oxygen-saturated supporting electrolyte at 25 °C

E_D (V)	$\overline{k_1}$ (cm^{-1})	$10^2\,\overline{k_2}$ (cm^{-1})	$10^4\,\overline{k_3}$ (cm^{-1})	E_D (V)	$10^3\,\overline{k_1}$ (cm^{-1})	$10\,\overline{k_2}$ (cm^{-1})	$10^4\,\overline{k_3}$ (cm^{-1})
0.60	0.754	0.18	–	0.38	1.21	0.80	2.22
0.62	0.348	0.84	–	0.36	1.37	1.24	2.25
0.64	0.343	0.94	–	0.34	7.31	1.41	2.24
0.66	0.230	1.66	–	0.32	13.6	1.59	2.50
0.68	0.190	2.63	3.6	0.30	21.4	1.91	2.73
0.70	0.130	5.60	4.0	0.28	10.2	2.54	2.83
0.72	0.089	5.62	4.1	0.26	8.1	3.63	2.86
0.74	0.048	4.74	3.5	0.24	7.0	4.57	3.06
0.76	0.003	2.56	2.3	0.22	5.2	5.75	3.08
0.78	0.002	1.94	1.3	0.20	2.9	6.42	3.11
0.80	–	1.47	1.5	0.18	1.2	8.83	3.54
0.82	–	0.78	0.9	–	–	–	–
0.84	–	0.69	0.7	–	–	–	–
0.86	–	0.43	0.4	–	–	–	–
0.88	–	0.22	0.2	–	–	–	–
0.90	–	0.17	0.1	–	–	–	–

showing that hydrogen peroxide is not consumed by a further electroreduction to water.

Conclusions

More knowledge about tin UPD on platinum is obtained by controlling the deposition variables, such as tin(II) ion concentration, deposition potential and deposition time. The application of a potentiodynamic cycling in the 0.05–0.60 V range in 10^{-4} M tin(II) acid solutions produces a surface rearrangement of tin ad-atoms to (110) sites and hydrogen ad-atoms to (100) sites.

The saturation surface coverage by tin on platinum is 2/3 without any irreversible adsorption. A Temkin isotherm is fitted for tin UPD on pc platinum and values of $\Delta G^{\circ}_{ad,\theta=0} = -420 \pm 40$ kJ mol^{-1} and $r = 13$ kJ mol^{-1} are calculated.

Rotating ring-disk electrode data for the OERR show the production of bulk hydrogen peroxide at tin UPD platinum, denoting a partial blockage of the reaction.

The reaction order with respect to oxygen varies with the nature of the surface. In the case of bare platinum, a dissociative oxygen reduction is demonstrated, whereas at tin UPD, a non-dissociative reduction producing bulk hydrogen peroxide is envisaged.

The interpretation of rotating ring-disk data based on Damjanovic's scheme indicates that molecular oxygen reduction at tin UPD platinum occurs through the formation of bulk hydrogen peroxide and water.

Acknowledgements The authors acknowledge the Programa para el Desarrollo de las Ciencias Básicas (PEDECIBA) Química for financial support (Uruguay). C.F.Z. is a researcher at PEDECIBA. G.O. has a fellowship granted by PEDECIBA.

References

1. Berenz P, Tillmann S, Massong H, Baltruschat H (1998) Electrochim Acta 43:3035
2. Massong H, Tillmann S, Langkau T, Abd El Meguid E, Baltruschat H (1998) Electrochim Acta 44:1379
3. Bakos I, Szabo S (2001) Electrochim Acta 46:2507
4. Xia XH (1999) Electrochim Acta 45:1057
5. Rodes A, Herrero E, Feliú JM, Aldaz A (1996) J Chem Soc Faraday Trans 92:3769
6. Bowles BJ (1966) Nature 212:1456
7. Bowles BJ, Cranshaw TE (1965) Phys Lett 17:258
8. Cadle SH, Brückenstein S (1971) Anal Chem 43:932
9. Shibata M, Furuya N (1989) J Electroanal Chem 269:217
10. Furuya N, Motoo S (1976) J Electroanal Chem 72:165
11. Szabo S (1984) J Electroanal Chem 172:359
12. Damjanovic A, Genshaw MA, Bockris JO'M (1964) J Chem Phys 45:4057
13. Park S-M, Ho S, Aruliah S, Weber M, Ward C, Venter R, Srinivasan S (1986) J Electrochem Soc 113:1641
14. Yeager E (1984) Electrochim Acta 29:1527
15. Adzic RR (1990) In: White RE, Bockris JO'M, Conway BE (eds) Modern aspects of electrochemistry, vol 21. Plenum Press, New York, pp 163–235
16. Kolb DM (1978) In: Gerisher H, Tobias CW (eds) Advances in electrochemistry and electrochemical engineering, vol.11 Interscience, New York, p 125
17. Ross PN, Andriacos PC (1983) J Electroanal Chem 154:205
18. Machado SAS, Tanaka AA, González ER (1991) Electrochim Acta 36:1325
19. Margheritis D, Salvarezza R, Giordano MC, Arvia AJ (1987) J Electroanal Chem 229:327
20. Zinola CF, Castro Luna AM, Triaca WE, Arvia AJ (1994) Electrochim Acta 39:1627
21. Zinola CF, Triaca WE, Arvia AJ (1995) J Appl Electrochem 25:740
22. Damjanovic A, Brusic V (1967) Electrochim Acta 12:615
23. Wroblowa H, Pan YC, Razumney G (1976) J Electroanal Chem 69:195
24. Angerstein-Kozlowska H (1984) In: Yeager EB, Bockris JO'M, Conway BE, Sarangapani S (eds) A comprehensive treatise of electrochemistry, vol 9. Plenum Press, New York, p 15